

SCPY 394: Advanced Physics Laboratory II

Lab 1: Measuring k_B from resistors

Dulyawat Boonvut, 6205110

September 18, 2022

1 Introduction

In conductors, a random motion from electrons leads to the appearance of noise (called Johnson's noise). In this experiment, we will measure the noise, from the random motion of electrons, of voltage on a resistor. Using different resistors with different resistance, Boltzmann constant k_B can be determined from this experiment.

2 Relevant Theory

Root mean square of noise from the resistor can be calculated by using

$$V_{rms} = \sqrt{4k_B T R \Delta f} \quad (1)$$

where

$k_B = 1.3806 \times 10^{-23} \text{ m}^2 \text{kg} \cdot \text{s}^{-2} \text{K}^{-1}$ is Boltzmann constant,

T is a temperature in K,

R is a resistance in Ω ,

Δf is a bandwidth, a specific range of used frequency, in Hz.

The experiment is designed to find the Boltzmann constant by measuring noise from resistors with different resistance. Doing the experiment together with using the equation (1) to analyze is applicable.

3 Part 0: Before the Experiment

The effective gain bandwidth f_e is used instead of Δf using the relation

$$f_e = \int_0^\infty |G(f)|^2 df \quad (2)$$

where $G(f)$ is a frequency-dependent gain (a ratio between the output voltage and input voltage to determine the amplification).

Hence equation (1) becomes

$$V_{rms} = \sqrt{4k_B T R f_e} \quad (3)$$

where f_e is determined by equation(4)

4 Part 1: Measuring frequency response and gain ratio

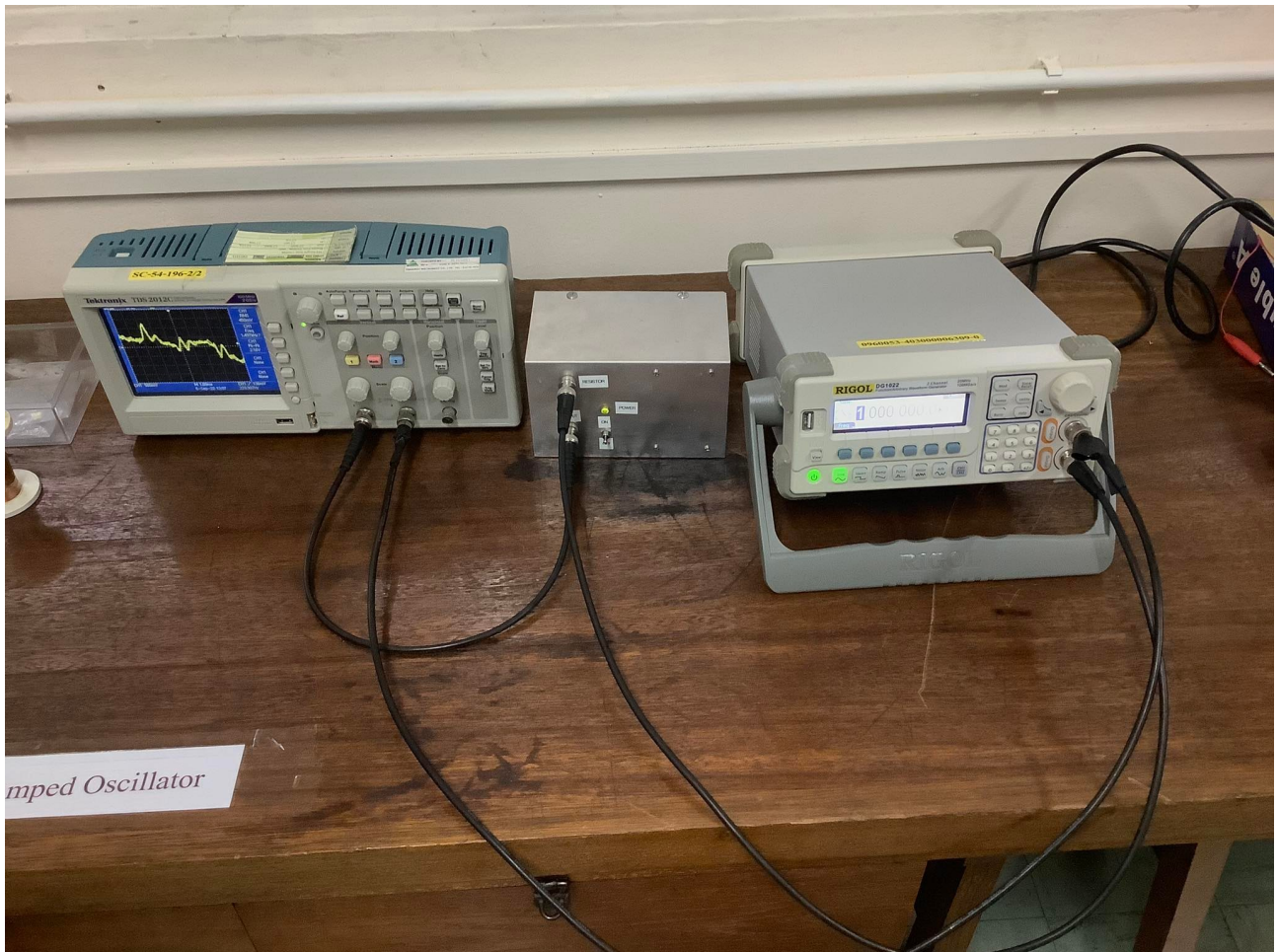


Figure 1: Experimental setup for part 1

The setup for part 1 (as shown in figure 1) consists of a function generator in which the sinusoidal signal is input into the system, an amplifier to amplify the signal (since the noise voltage is significantly small), and an oscilloscope for measuring different values from the amplified signal.

We fix the input amplitude of the wave at $V_{in} = 4.0 \text{ mV}$. We then measure the output signal V_{out} as a root mean square (RMS) voltage measure by using a "Measure" mode in the oscilloscope.

Different frequencies will show the different V_{out} and also show different gain $G = V_{out}/V_{in}$, as shown in the below table.

f (Hz)	G (± 1)
10	104
20	105
40	132
70	1596
100	2745
200	6063
400	9581
700	11402
1000	12021
2000	12410
4000	12198
7000	11455
10000	10430
20000	7372
40000	3730
70000	1566
100000	804
200000	222

Table 1: Data table for part 1

A graph of frequency and square of gain is shown below.

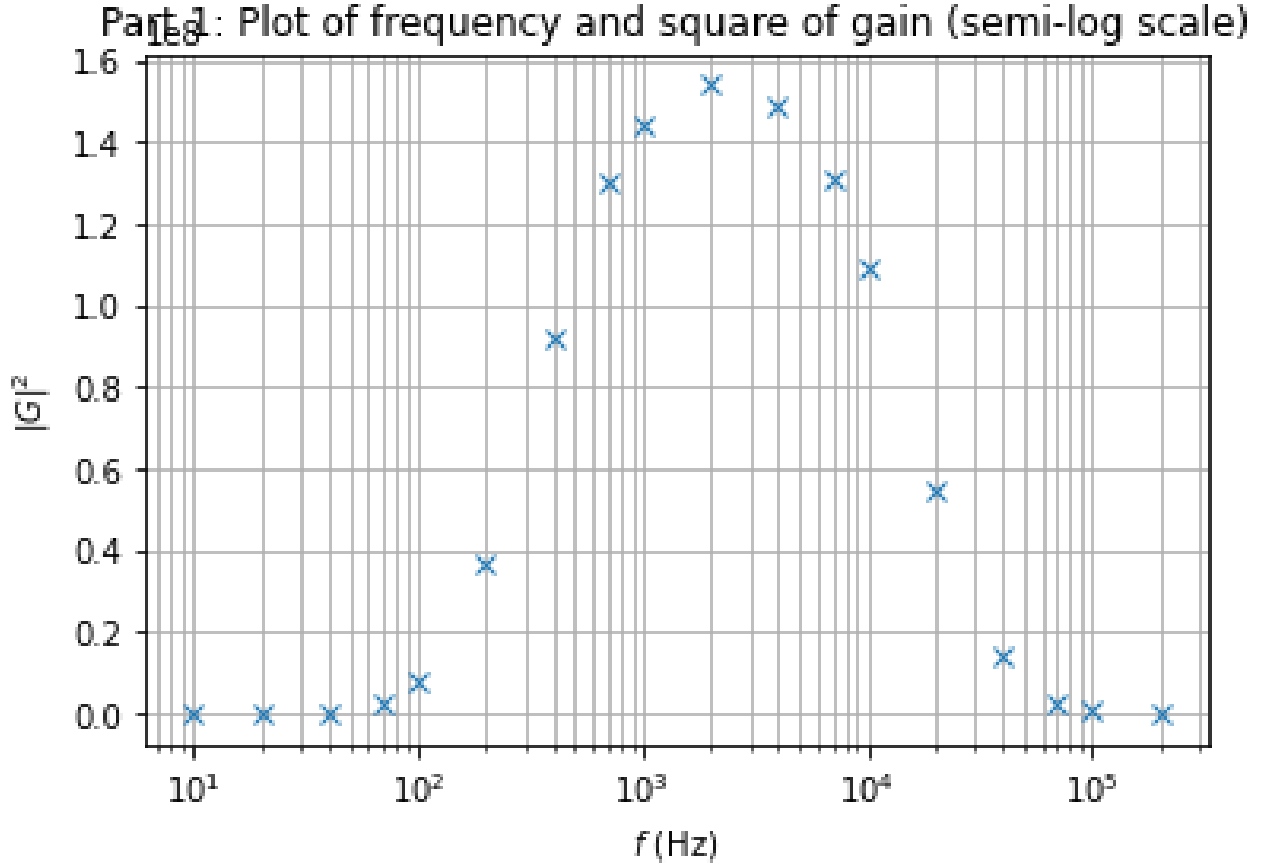


Figure 2: Graph of frequency and gain (Part 1)

From the graph 2, we can calculate the integral. We therefore use Simpson's rule for integration of an array of data evaluated by Python and we obtain

$$f_e = \int_0^\infty |G(f)|^2 df = (2.90 \pm 0.01) \times 10^{12} \text{ Hz} \quad (4)$$

5 Part 2: Measuring voltage from the noise of resistors

In part 2, the function generator is excluded. Replacing with a portable circuit with a resistor, it can determine noise voltage V_n . When using $R = 0$ circuit, the noise still appears and discrepancy exists since $V = 0$ when $R = 0$ (from equation (1)).

In this experiment, we obtained $V(R = 0) = 122 \pm 1$ V.

From the experiment, data is shown in the below table

R (Ω)	V_{rms} (± 1 mV)	V_n (± 1 mV)
47	123	1
100	123	1
220	123	1
470	122	1
1000	122	1
2200	124	2
4700	126	4
10000	130	8
22000	138	16
47000	152	30
100000	164	42
220000	200	78
470000	260	138
1000000	320	198

Table 2: Data table for part 2

The graph of resistance and noise voltage is shown below.

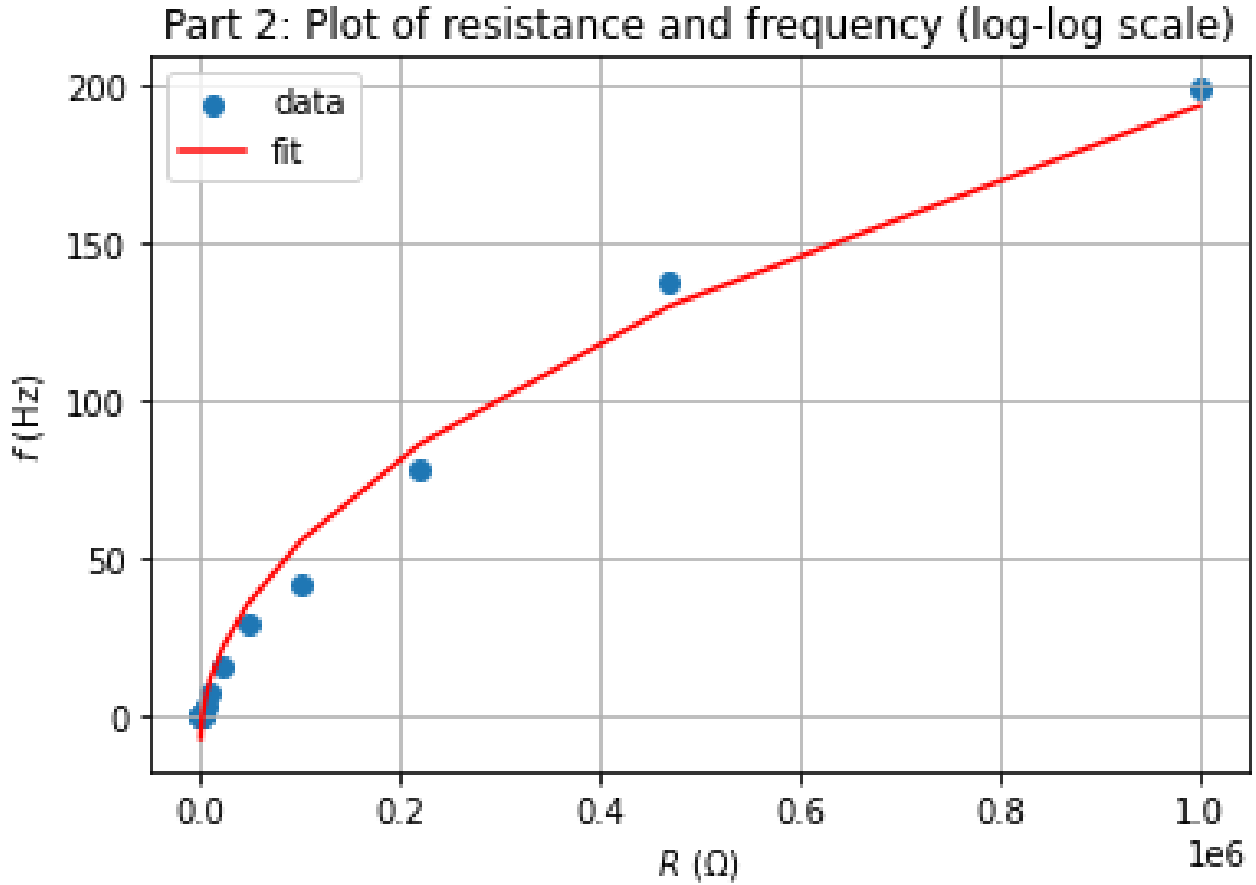


Figure 3: Graph of resistance and noise voltage (Part 2)

6 Part 3: Data Analysis

The data from the table 2 can be used for finding the value of the Boltzmann constant. Using the objective equation $V_{rms} = \sqrt{\alpha R}$, we obtain

$$\alpha = (4052 \pm 6) \times 10^{-6} \text{ mV}^2/\Omega \quad (5)$$

From equation (1), $\alpha = 4k_B T f_e$, we therefore obtain $k_B = \alpha / (4T f_e)$

Hence the Boltzmann constant is

$$k_B = (1.2 \pm 0.2) \times 10^{-23} \text{ V}^2/(\Omega \cdot \text{K} \cdot \text{Hz}) \quad (6)$$

The real value of k_B is

$$k_B \approx 1.3801 \times 10^{-23} \text{ m}^2 \text{kg} \cdot \text{s}^{-2} \text{K}^{-1} \quad (7)$$

The exact result covers inside the boundary of the obtained value from the experiment.

SCPY 394: Advanced Physics Laboratory II

Lab 2: Four-Point-Probe Conductivity Measurement

Dulyawat Boonvut, 6205110

September 13, 2022

1 Objective

To find the sheet resistivity using **Collinear Four-Point Probe method** and **van der Pauw method**.

2 Sheet Resistance

The resistance R of a conductive sheet with width w , length L and thickness t , and resistivity ρ is

$$R = \frac{\rho L}{tW} \quad (1)$$

Since R is shape-dependent (depend on the dimension of the object), we define

$$R_s = \frac{\rho}{t} \quad (2)$$

as **sheet resistance** which is material-dependent but shape-independent.

3 Collinear Four-Point Probe method

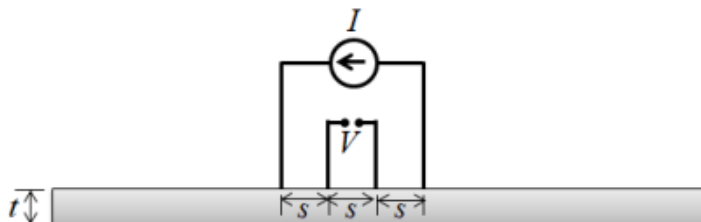
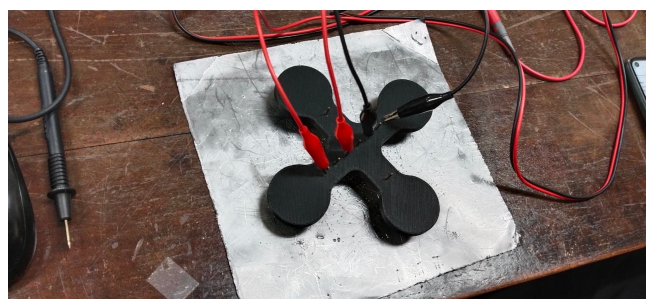


Figure 1: Illustration of implementing collinear four-point probe method (From lab manual)



6

Figure 2: Experimental setup for collinear four-point probe method

Using two points connecting with a current source and two points connecting a coordinate in the boundary of the object, we can measure the resistance of the object, as shown in figure 2. In this experiment, graphite which the resistivity is $\rho = 1380 \times 10^{-8} \Omega \cdot \text{m} = 1.380 \times 10^{-5} \Omega \cdot \text{m}^1$ is used.

¹From <http://www.troelsgravesen.dk/graphite.htm>

With thin film ($t \ll s$),

$$R_s = \frac{\rho}{t} = \frac{\pi}{\ln(2)} \frac{V}{I} \quad (3)$$

Rearranging equation(3) to obtain

$$V = \frac{\rho \ln(2)}{\pi t} I \quad (4)$$

which we can collect the data of V with some chosen I using the setup shown in figure 2. We find the resistivity of sheets with different shapes: big square sheet, small square sheet, and circular sheet, all with $t = 0.5$ mm. Fitting the linear equation (4), we can obtain the resistivity by considering its slope (that is $\rho = \frac{(\text{SLOPE})\pi t}{\ln(2)}$).

The raw data table is shown below. V_{big} is the voltage measured at the bigger square sheet, V_{square} is the voltage measured at the smaller square sheet, and V_{circle} is the voltage measured at the circular sheet.

I (± 0.001 A)	V_{big} (± 0.002 mV)	V_{square} (± 0.002 mV)	V_{circle} (± 0.002 mV)
0.600	2.978	6.367	5.562
0.620	3.086	6.563	5.743
0.640	3.194	6.776	5.926
0.660	3.287	6.988	6.110
0.680	3.392	7.197	6.295
0.700	3.470	7.410	6.475
0.720	3.576	7.615	6.656
0.740	3.733	7.822	6.836
0.760	3.813	8.033	7.017
0.780	3.866	8.236	7.197
0.800	3.943	8.443	7.374
0.820	4.076	8.656	7.533
0.840	4.168	8.852	7.710
0.860	4.253	9.047	7.879
0.880	4.330	9.236	8.043
0.900	4.361	9.427	8.209
0.920	4.495	9.620	8.371
0.940	4.573	9.809	8.540
0.960	4.652	10.006	8.707
0.980	4.741	10.190	8.873
1.000	4.763	10.414	9.047

Table 1: Raw data table from collinear four-point probe method

From the data, the V - I graph for different shapes are shown below

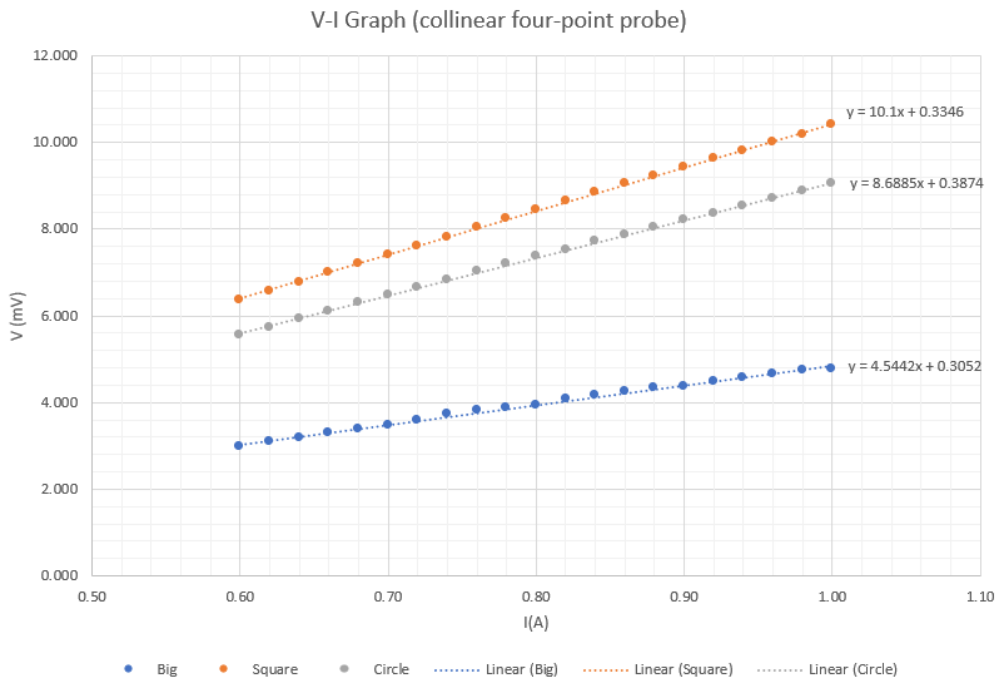


Figure 3: V - I graph (collinear four-point probe)

From the graph, its slope and resistivity is shown below

Object	slope (Ω)	ρ ($\Omega \cdot \text{m}$)
Big rectangular sheet	4.54 ± 0.07	$(2.29 \pm 0.02) \cdot 10^{-5}$
Square sheet	10.10 ± 0.04	$(1.97 \pm 0.01) \cdot 10^{-5}$
Circular sheet	8.69 ± 0.04	$(1.029 \pm 0.004) \cdot 10^{-5}$

Table 2: Slope and resistivity

In comparison with the known resistivity of graphite, the smaller sheet results better in measuring resistivity by using collinear four-point probe.

4 Van der Pauw method

Using the setup like one using the collinear four-point probe with different configuration of probe connection as shown in figure 4, we can determine the potential different V_i in i^{th} configuration, called the van der Pauw method. The result is expected to be better than one with the collinear four-point probe method since the van der Pauw method is area-dependent, that area of the object affects the different results of voltage.

The raw data table of V at different configurations for square and circular sheets is shown below.

V_i	V_{square} (± 0.002 mV)	V_{circle} (± 0.002 mV)
V_1	4.323	4.201
V_2	-4.652	-4.523
V_3	4.258	4.923
V_4	-4.583	-5.263
V_5	4.285	4.195
V_6	-4.645	-4.532
V_7	4.230	4.915
V_8	-4.595	-5.261

Table 3: Raw data table from van der Pauw method

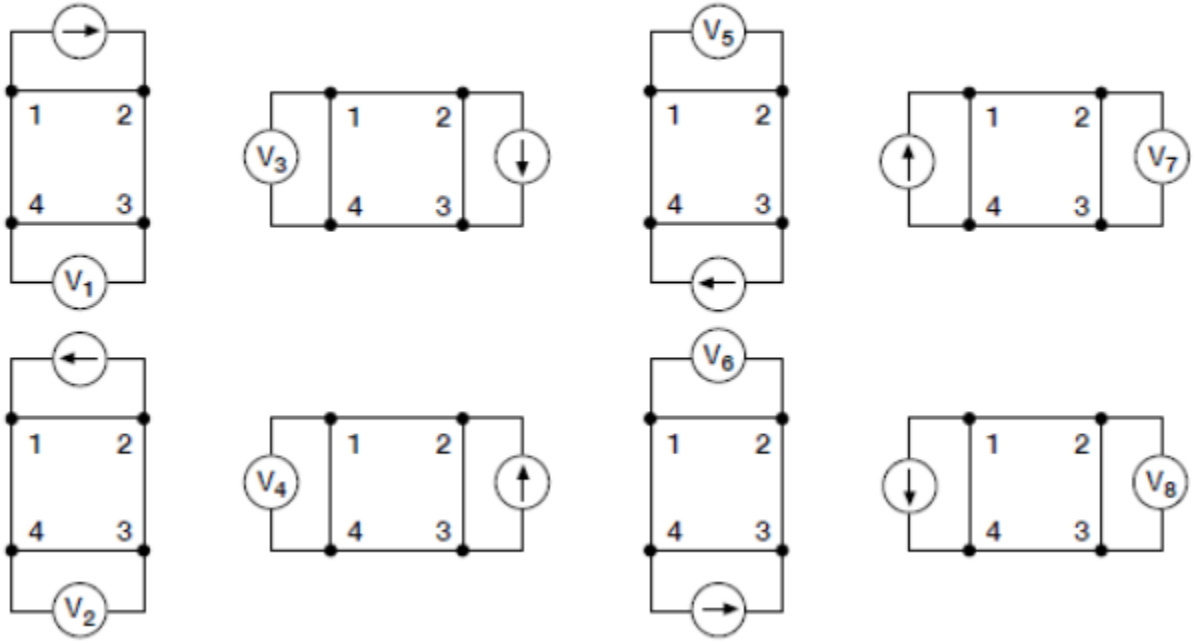


Figure 4: Configurations of probe connection (From: lab manual)

From the van der Pauw method, the resistivity ρ is calculated using the following equations.

$$\begin{cases} \rho_a = \frac{\pi}{\ln(2)} f_a t \frac{V_1 - V_2 + V_3 - V_4}{4I} \\ \rho_b = \frac{\pi}{\ln(2)} f_b t \frac{V_5 - V_6 + V_7 - V_8}{4I} \\ \rho = \frac{\rho_a + \rho_b}{2} \end{cases} \quad (5)$$

where f_i ($i = A, B$) is the solution of

$$\frac{Q_i - 1}{Q_i + 1} = \frac{f_i}{0.693} \cosh^{-1} \left(\frac{e^{0.693/f_i}}{2} \right) \quad (6)$$

where

$$Q_i = \begin{cases} \frac{V_1 - V_2}{V_3 - V_4} & \text{if } i = A \\ \frac{V_5 - V_6}{V_7 - V_8} & \text{if } i = B \end{cases} \quad (7)$$

Using the van der Pauw method, resistivity ρ is

Object	ρ ($\Omega \cdot \text{m}$)
Square sheet	$(1.007 \pm 0.002) \cdot 10^{-5}$
Circular sheet	$(1.07 \pm 0.01) \cdot 10^{-5}$

Table 4: Table of calculated values including the resulting resistivity

From the values in the aforementioned table, the van der Pauw method shows better results than the collinear four-point probe since the reported value is nearly to the known resistivity of graphite.

SCPY 394: Advanced Physics Laboratory II

Lab 3: Circular Diffraction

Dulyawat Boonvut, 6205110

September 27, 2022

1 Objective

To observe circular diffraction using a laser from an optical fiber.

2 Experiment and Result

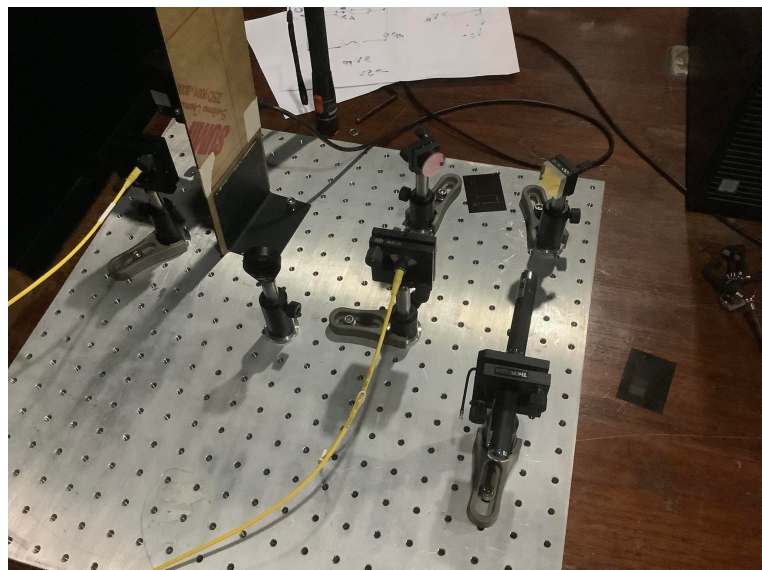


Figure 1: Experimental Setup

An apparatus for this experiment consists of an optical fiber, two reflectors, a Linear CCD module (sensor to detect and connect with a personal computer), and some circle apertures.

From the setup shown in figure 1, replace an output optical fiber with a green laser. The green laser is used for aligning the input red laser. After the alignment finishes, replace the optical fiber back to the collimator. The light from the input laser is then adjusted to align with the linear CCD.

When the setup is finished as shown in figure 1, the diffraction pattern from the light source must be shown on the monitor. However, the pattern is invisible. We see no pattern on the screen.

However, we try pointing the laser to the Linear CCD to observe the error of the output receiver. The result is shown below.

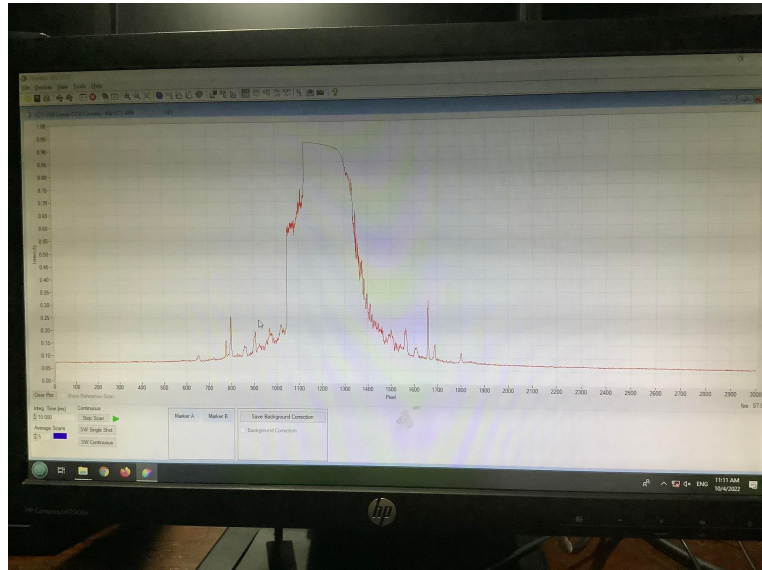


Figure 2: Result with direct input light

3 Conclusion

The experiment is to observe circular diffraction by doing the light adjustment. The result with direct light input shows an intensity graph quite well; however, the result when doing the pre-explained setup shows no pattern in the output. Many reasons are proposed: internal damage to the optical fiber, lack of laser intensity to affect CCD sensitivity, a mistake in light adjustment.

SCPY 394: Advanced Physics Laboratory II

Lab 4: Lock-In Amplification

Dulyawat Boonvut, 6205110

October 25, 2022

1 Objective

To study basic Lock-In detection technique, working principle of Lock-In Amplifier, and its application.

2 Theories

The Lock-In detection technique is phase-sensitive detection; the signal component in phase with a reference signal is measured by using an input signal

$$V_{sig}(t) = V_{sig}^0 \sin(2\pi ft + \theta) \quad (1)$$

,same frequency f as the reference signal

$$V_{ref}(t) = V_{ref}^0 \sin(2\pi ft) \quad (2)$$

but with phase difference θ .

For the Lock-In Amplifier used in the experiment, DSP Lock-In Amplifier Model SR830, the signal voltage is measured in in-phase component $X(t) = V_{sig}^0 \cos(\theta)$ and quadrature component $Y(t) = V_{sig}^0 \sin(\theta)$ with amplitude $R(t) = \sqrt{X^2(t) + Y^2(t)} = V_{sig}^0$ and phase difference from the reference signal $\theta = \arctan \frac{Y(t)}{X(t)}$

3 Capacitance measurement using Lock-In Amplifier

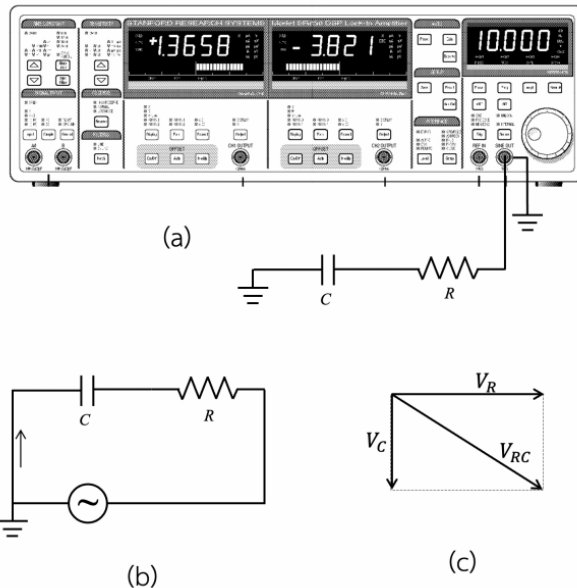


Figure 1: Circuit representation for using Lock-In Amplifier to measure capacitance

The sub-experiment is to measure capacitance by using the Lock-In Amplifier instead of an ordinary method using a multimeter. We connect a sine-wave source to an R-C circuit as shown in figure 1. The voltage between a capacitor is used as an input of the Lock-In Amplifier. The complete setup is shown in figure 2.



Figure 2: The experimental setup for using Lock-In Amplifier to measure capacitance

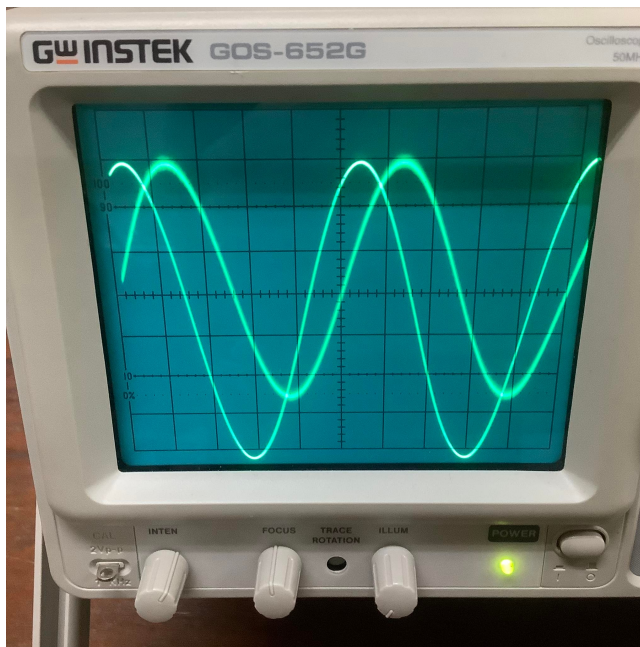


Figure 3: The result signals from the R-C circuit

From the setup, the result signals are shown in figure 3

From figure 1, measured quantities from the Lock-in Amplifier are shown in the below table.

Quantities from Lock-In Amplifier	Quantities from phasor diagram
X	voltage between capacitor V_C
Y	voltage between resistor V_R
R	source voltage V_{RC}
θ	phase difference between V_C and V_{RC}

Table 1: Comparison of quantities from Lock-In Amplifier and quantities from phasor diagram

Using a frequency range of 1 to 10 kHz, the obtained data is represented in the below graph.

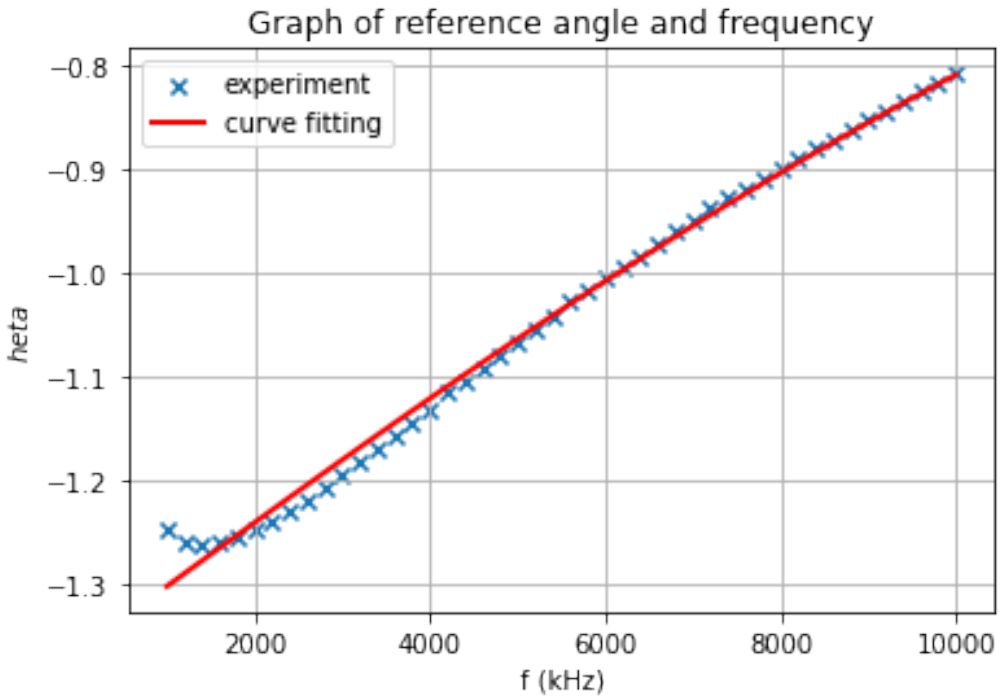


Figure 4: Graph of θ and frequency of the R-C circuit

From the prior knowledge of AC circuits, θ can be obtained from frequency.

$$\theta(f) = \arctan(2\pi RCf) + \theta_0 \quad (3)$$

where θ_0 is the reference phase, different for a unique system.

In the sub-experiment, $R = 47 \Omega$. With curve fitting, the capacitance is

$$C = 209 \pm 3 \text{ nF}$$

4 Lock-In detection technique to measure noise-rich signal

The sub-experiment is to modulate the noise-rich signal. We compare using a multimeter with using a Lock-In Amplifier to examine both efficiencies.

4.1 Multimeter

We connect an electric source to a circuit (+5V). A non-zero output voltage, called **offset voltage** V_{off} , is expected even if electricity is unavailable in the system. In the sub-experiment, the offset voltage

$$V_{\text{off}} = 4.7 \pm 0.1 \text{ mV} \quad (4)$$

Then the source is connected to the 2.0 V LED. From the observation, the voltage is $251 \pm 1 \text{ mV}$ and it increases from V_{off} for

$$V_0 - V_{\text{off}} = 246 \pm 1 \text{ mV} \quad (5)$$

In the sub-experiment, a light-attenuated sheet is added to the system. The expected measured voltage must decrease when the number of sheets increases. For the number of sheets, the output voltage V_{out} is in the same order as the offset voltage, so the multimeter will be inapplicable.

From the sub-experiment, a graph of $V_{\text{out}} = V - V_{\text{off}}$ with a different number of sheets is shown below.

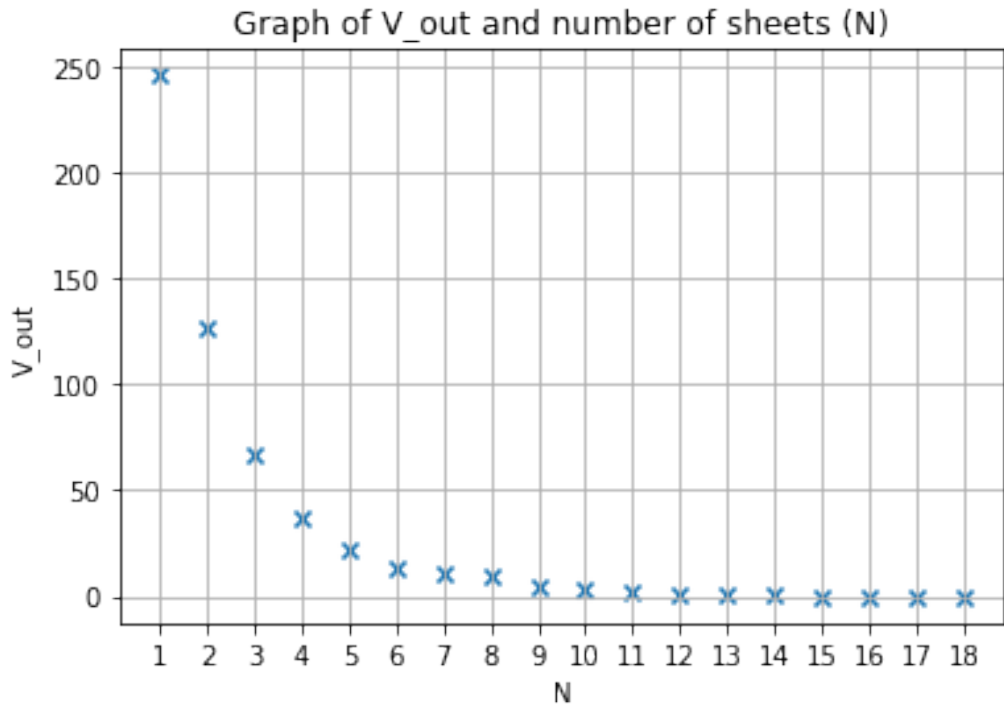


Figure 5: graph of V_{out} and number of sheets

From the graph 5, the multimeter measurement is inapplicable when the number of sheets exceeds $N = 14$.

4.2 Lock-In Amplifier

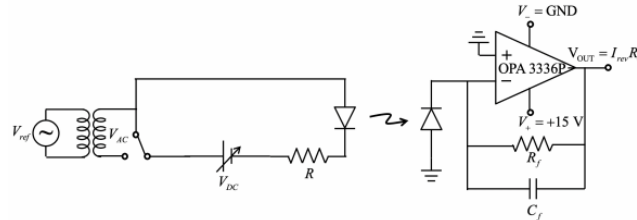


Figure 6: Circuit representation for noise-rich signal modulation in LED circuit

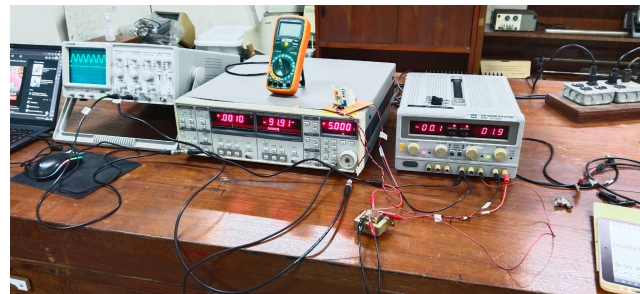


Figure 7: The experimental setup for noise-rich signal modulation in LED circuit

With the setup 7, with a change of output voltage from the multimeter to the Lock-In Amplifier input, the same output voltage can be observed with a different number of sheets. The corresponding output from the Lock-In amplifier to analyze further is Y .

The graph of Y and the number of sheets is shown below

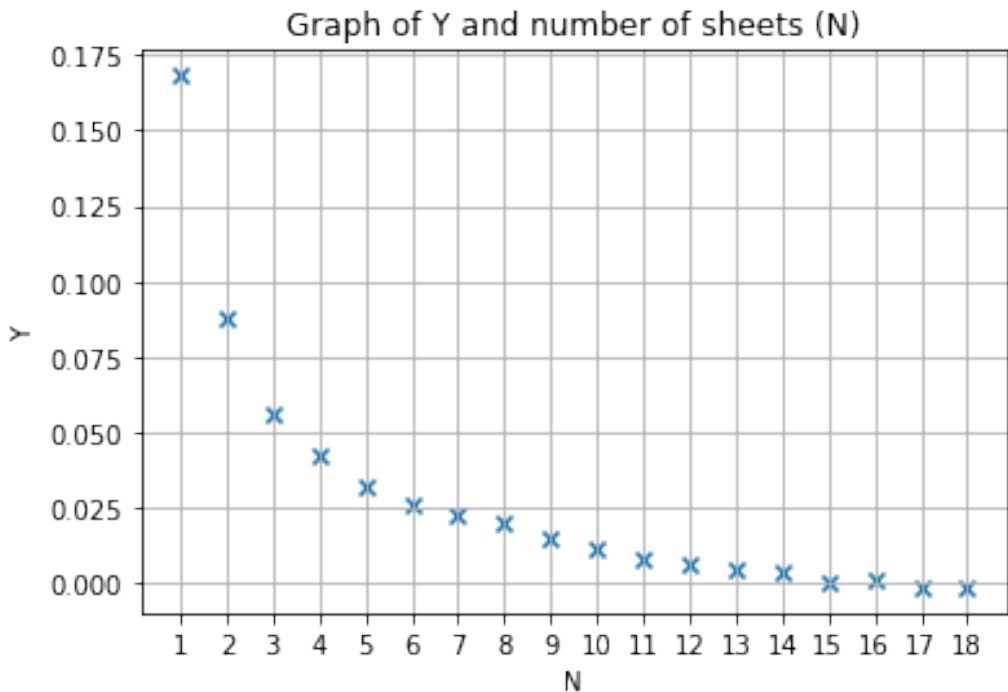


Figure 8: graph of Y and the number of sheets using the Lock-In Amplifier

From graph 8, the Lock-In Amplifier measurement is inapplicable when the number of sheets exceeds $N = 16$.

5 Conclusion

The experiment is to use a Lock-In Amplifier in various scenarios. In a resistor-capacitor system, we can obtain the capacitor by using the Lock-In Amplifier $C = 209 \pm 3 \text{ nF}$. With measuring a noise-rich signal of an LED circuit, the comparison using a multimeter and a Lock-In Amplifier is conducted. The resulting number of sheets that the voltage measurement is inapplicable from the multimeter is $N \geq 14$ whereas one from the Lock-In Amplifier is $N \geq 16$

SCPY 394: Advanced Physics Laboratory II

Lab 5: Long-time data collecting using LabVIEW

Dulyawat Boonvut, 6205110

September 13, 2022

1 Objective

To use LabVIEW to do long-time automatic data acquisition to measure liquid temperature and observe the water melting and the water cooling phenomena.

2 Measuring temperature using thermistor

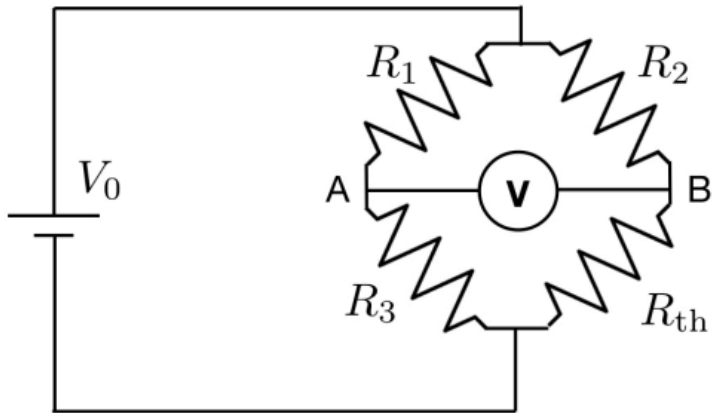


Figure 1: Circuit used in the experiment to measure the temperature

Using electric signal obtained from the bridge circuit in figure 1, voltage between the thermistor is

$$V = V_A - V_B = V_0 \left(\frac{R_3}{R_3 + R_1} - \frac{R_{th}}{R_{th} + R_2} \right) \quad (1)$$

For each thermistor voltage V_{th} obtained from the automatic data acquisition, the temperature T can be determined by applying equation (1) to solve for thermistor resistance R_{th} and then using the below fitted function from the table in the appendix to compute the temperature T .

$$T = A + B \ln(R_{th}) + C \ln^3(R_{th}) \quad (2)$$

where $A = 347.8 \pm 0.6$, $B = -41.1 \pm 0.1$ and $C = (7.21 \pm 0.06) \times 10^{-2}$ are parameters from the thermistor data.

3 Using LabVIEW (LV)

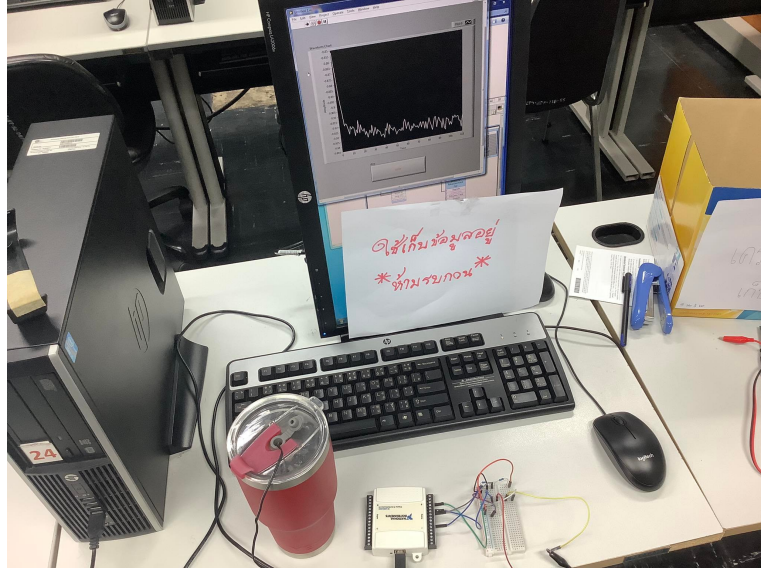


Figure 2: The experimental setup

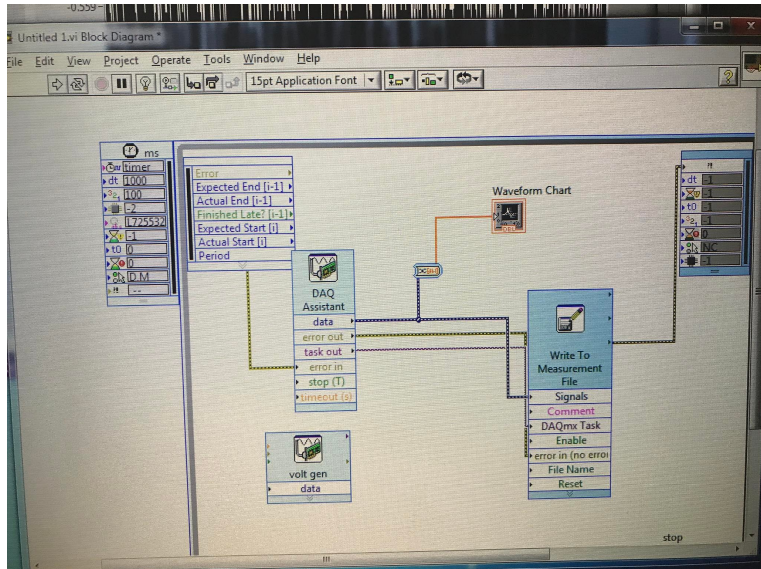


Figure 3: LV code used in the experiment

LabVIEW (LV) is a simple programming language using visual code (figures) instead of typical alphabetical code. In the experiment, LV is used for long-time data collecting. By connecting the USB-6009 with the circuit connected same as figure 1 with $R_1 = R_2 = R_3 = 3.3 \text{ k}\Omega$ to a personal computer. The complete setup is shown in figure 2. LV code is implemented, shown in figure 3, to collect the data of voltage. Voltage will be transformed to thermistor resistor by using equation (1) and temperature afterward by using table in the appendix.

4 Comparative result with Newton's Law of Cooling

A system with time-dependent temperature is governed by Newton's law of cooling, where temperature T evolves as time t passes by:

$$\frac{dT}{dt} = A(T_R - T) \quad (3)$$

where T_R is a surrounding temperature, and A is constant depending on the system.

In this experiment, there are two data sets, one with the cooling of hot water and another one with the melting of iced water. Both systems are in an insulated container. The data from the system is collected using LV and then compared with a numerically exact solution of Newton's law of cooling.

4.1 Cooling of hot water in an insulated container

Using hot water along with the circuit set as in figure 1, the data is collected and shown as a graph below. The graph also contains a numerical result from Newton's law of cooling (3). The obtained result is consistent with

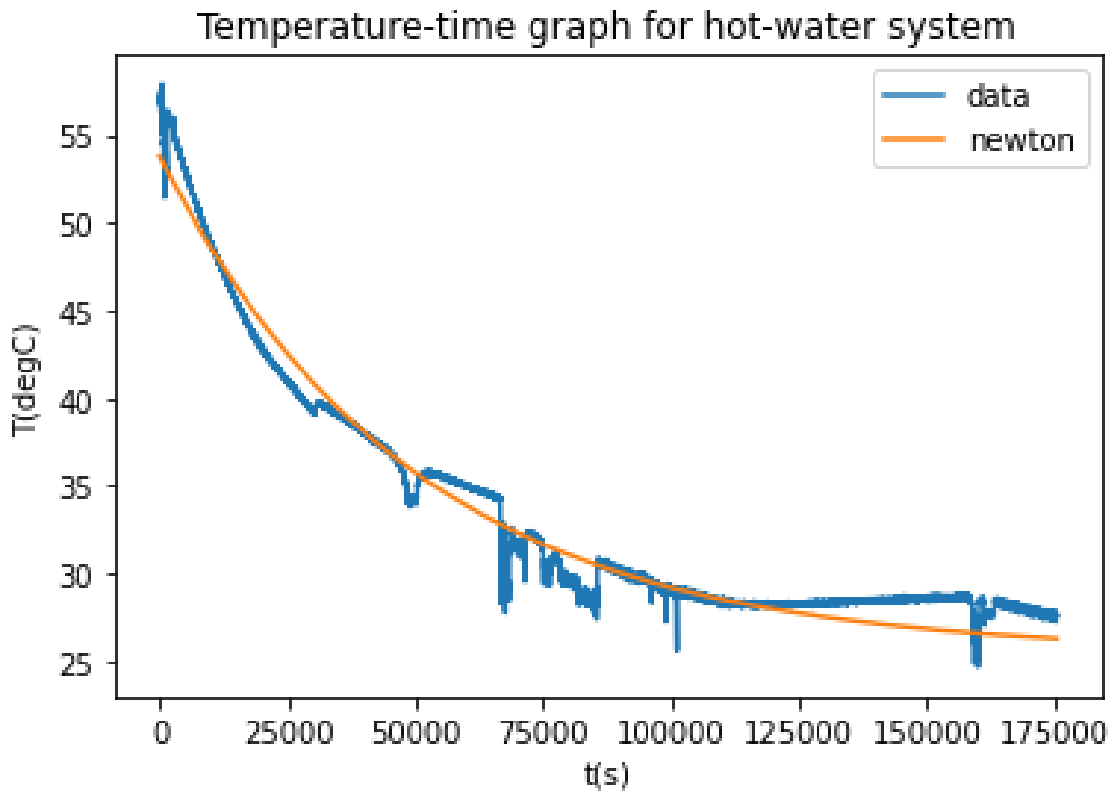


Figure 4: Temperature-time graph of the hot water system

Newton's law of cooling with $A_{hot} = (2.031 \pm 0.004) \times 10^{-5} \text{s}^{-1}$

4.2 Melting of iced water in an insulated container

Using iced water along with the circuit set as in figure 1, the data is collected and shown as a graph below. The graph also contains a numerical result from Newton's law of cooling (3). Considering at temperature-changing

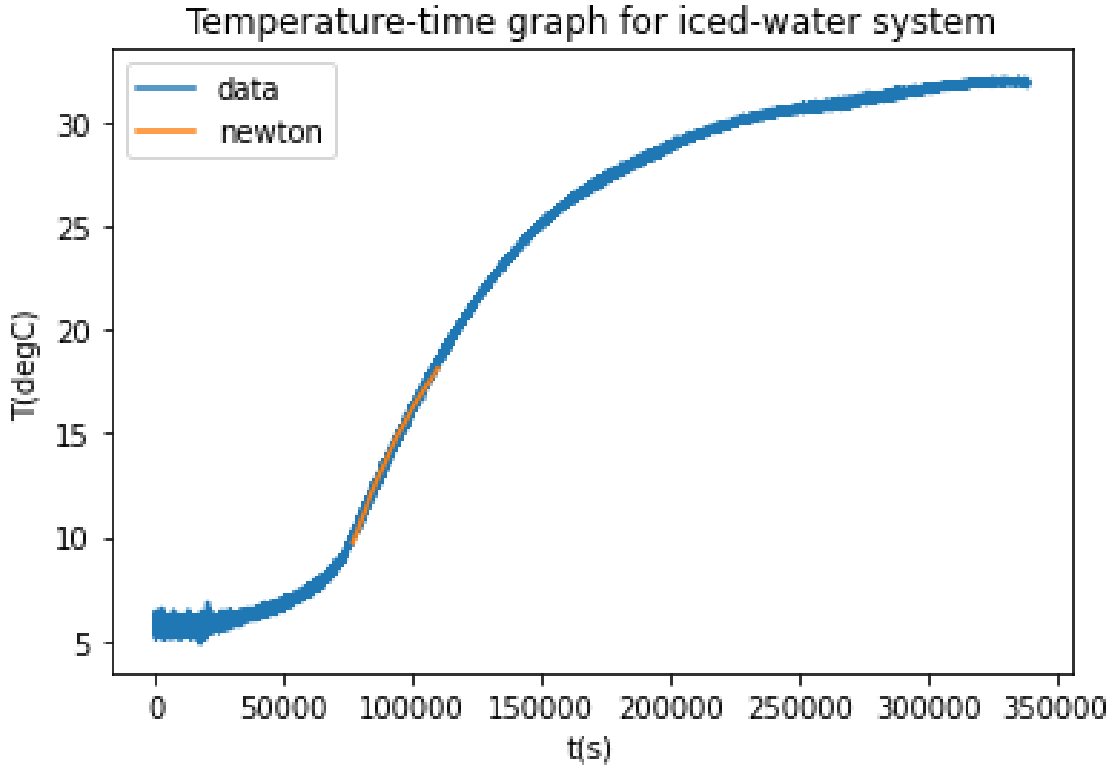


Figure 5: Temperature-time graph of the iced water system

phase, the obtained result is consistent with Newton's law of cooling with $A_{ice} = (2.479 \pm 0.004) \times 10^{-5} \text{s}^{-1}$

5 Conclusion

The experiment is to observe the cooling and melting phenomena. LabVIEW is used for long-time data acquisition in the experiment. For the cooling of hot water, the constant of Newton's law of cooling is $A_{hot} = (2.031 \pm 0.004) \times 10^{-5} \text{s}^{-1}$ whereas A for the melting of iced water is $A_{ice} = (2.479 \pm 0.004) \times 10^{-5} \text{s}^{-1}$

6 Appendix: Resistor-temperature table for the thermistor

T (°C)	R (Ω)								
0.0	32624.2	20.0	12492.8	40.0	5323.9	60.0	2483.8	80.0	1251.8
0.5	31804.3	20.5	12214.2	40.5	5217.9	60.5	2439.5	80.5	1231.6
1.0	31007.3	21.0	11942.6	41.0	5114.4	61.0	2396.0	81.0	1211.8
1.5	30232.8	21.5	11677.8	41.5	5013.2	61.5	2353.4	81.5	1192.4
2.0	29479.8	22.0	11419.7	42.0	4914.2	62.0	2311.7	82.0	1173.4
2.5	28747.9	22.5	11168.0	42.5	4817.5	62.5	2270.9	82.5	1154.6
3.0	28036.4	23.0	10922.5	43.0	4722.9	63.0	2230.8	83.0	1136.3
3.5	27344.5	23.5	10683.2	43.5	4630.5	63.5	2191.6	83.5	1118.2
4.0	26671.8	24.0	10449.8	44.0	4540.1	64.0	2153.2	84.0	1100.5
4.5	26017.6	24.5	10222.1	44.5	4451.7	64.5	2115.6	84.5	1083.2
5.0	25381.4	25.0	10000.0	45.0	4365.3	65.0	2078.7	85.0	1066.1
5.5	24762.6	25.5	9783.4	45.5	4280.8	65.5	2042.5	85.5	1049.4
6.0	24160.7	26.0	9572.0	46.0	4198.1	66.0	2007.0	86.0	1032.9
6.5	23575.3	26.5	9365.9	46.5	4117.3	66.5	1972.3	86.5	1016.8
7.0	23005.7	27.0	9164.7	47.0	4038.2	67.0	1938.3	87.0	1000.9
7.5	22451.6	27.5	8968.5	47.5	3960.9	67.5	1904.9	87.5	985.3
8.0	21912.5	28.0	8777.0	48.0	3885.2	68.0	1872.2	88.0	970.0
8.5	21387.8	28.5	8590.1	48.5	3811.2	68.5	1840.1	88.5	955.0
9.0	20877.3	29.0	8407.7	49.0	3738.8	69.0	1808.7	89.0	940.3
9.5	20380.5	29.5	8229.7	49.5	3668.0	69.5	1777.9	89.5	925.8
10.0	19896.9	30.0	8056.0	50.0	3598.7	70.0	1747.7	90.0	911.6
10.5	19426.2	30.5	7886.4	50.5	3530.9	70.5	1718.0	90.5	897.6
11.0	18968.0	31.0	7720.8	51.0	3464.6	71.0	1689.0	91.0	883.9
11.5	18522.0	31.5	7559.2	51.5	3399.7	71.5	1660.5	91.5	870.4
12.0	18087.8	32.0	7401.4	52.0	3336.1	72.0	1632.6	92.0	857.2
12.5	17664.9	32.5	7247.4	52.5	3273.9	72.5	1605.2	92.5	844.2
13.0	17253.2	33.0	7097.0	53.0	3213.1	73.0	1578.3	93.0	831.4
13.5	16852.3	33.5	6950.1	53.5	3153.5	73.5	1552.0	93.5	818.8
14.0	16461.9	34.0	6806.6	54.0	3095.2	74.0	1526.1	94.0	806.5
14.5	16081.6	34.5	6666.6	54.5	3038.1	74.5	1500.8	94.5	794.4
15.0	15711.3	35.0	6529.7	55.0	2982.3	75.0	1475.9	95.0	782.5
15.5	15350.5	35.5	6396.1	55.5	2927.6	75.5	1451.5	95.5	770.8
16.0	14999.0	36.0	6265.6	56.0	2874.0	76.0	1427.6	96.0	759.3
16.5	14656.6	36.5	6138.1	56.5	2821.6	76.5	1404.2	96.5	748.0
17.0	14323.0	37.0	6013.5	57.0	2770.3	77.0	1381.1	97.0	736.9
17.5	13998.0	37.5	5891.8	57.5	2720.0	77.5	1358.5	97.5	725.9
18.0	13681.2	38.0	5772.9	58.0	2670.8	78.0	1336.4	98.0	715.2
18.5	13372.5	38.5	5656.7	58.5	2622.6	78.5	1314.6	98.5	704.7
19.0	13071.7	39.0	5543.2	59.0	2575.3	79.0	1293.3	99.0	694.3
19.5	12778.5	39.5	5432.3	59.5	2529.1	79.5	1272.4	99.5	684.1

Figure 6: Resistor-temperature table of the thermistor. From: SCPY393 Lab Direction

SCPY 394: Advanced Physics Laboratory II

Lab 6: Density Functional Theory (DFT) calculation

Dulyawat Boonvut, 6205110

November 23, 2022

1 Objective

1. To find lattice constants of aluminum and silicon.
2. To obtain a density state representation from a band structure from different materials.
3. To study van Hove singularity from the band structures of the different materials.

2 Density Functional Theory (DFT)

Density functional theory (DFT) uses a **density functional** instead of a typical wave function. Using the density functional, material properties can be determined. With the appropriate density functional, ground state energy can be determined by the variational principle.

3 Calculation Process using DFT

The density function is usually determined by **self-consistent method** which an initial density functional is constructed from a non-interactive system and the corresponding energy will be calculated. The density function will be reconstructed and used for a calculation repeatedly until the energy converges to a specific value.

The used model in the experiment is **muffin-tin orbital model**, which atom is inside the *muffin tin*. Spherical harmonics as a basis function will contribute to the density function to obtain the ground state energy using a self-consistent method.

Each material has a unique lattice constant. The lattice constant can be obtained using the self-consistent method. For different samples of lattice constant, cohesive energy is obtained for the number of iterations. We can then determine the actual value of the lattice constant by considering the lowest cohesive energy.

The obtained lattice constant will be used to obtain a band structure. the density of state (DOS) - energy graph will be shown also.

The experiment focuses on the materials: *aluminum* and *silicon*. Their lattice constants are obtained and their band structures afterward. The van Hove singularities of both materials, which are represented as spikes in the DOS graph, are observed.

4 Results

4.1 Result of aluminum

4.1.1 Lattice constant

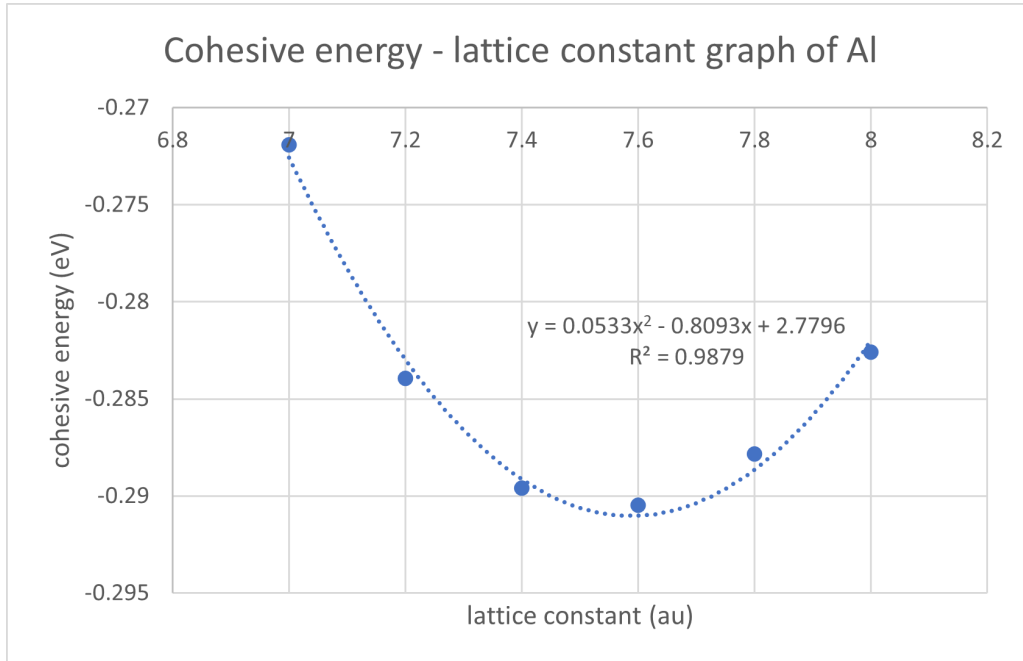


Figure 1: Lattice constant - cohesive energy graph of aluminum

From figure 1, the lattice constant of aluminum corresponding to the lowest cohesive energy is

$$a_{Al} = 7.597 \text{ au} = 4.019 \text{ \AA} \quad (1)$$

The obtained aluminum lattice constant is approximately close to $a = 404.95 \text{ pm} = 4.0495 \text{ \AA}$ from <https://periodictable.com/Elements/013/data.html>.

4.1.2 Density of state

from figure 6 An amount of peculiar peaks along the continuous line of graph 6 represent **van Hove singularities**. The van Hove singularities show possible state of the material since number of state is rapidly changing.

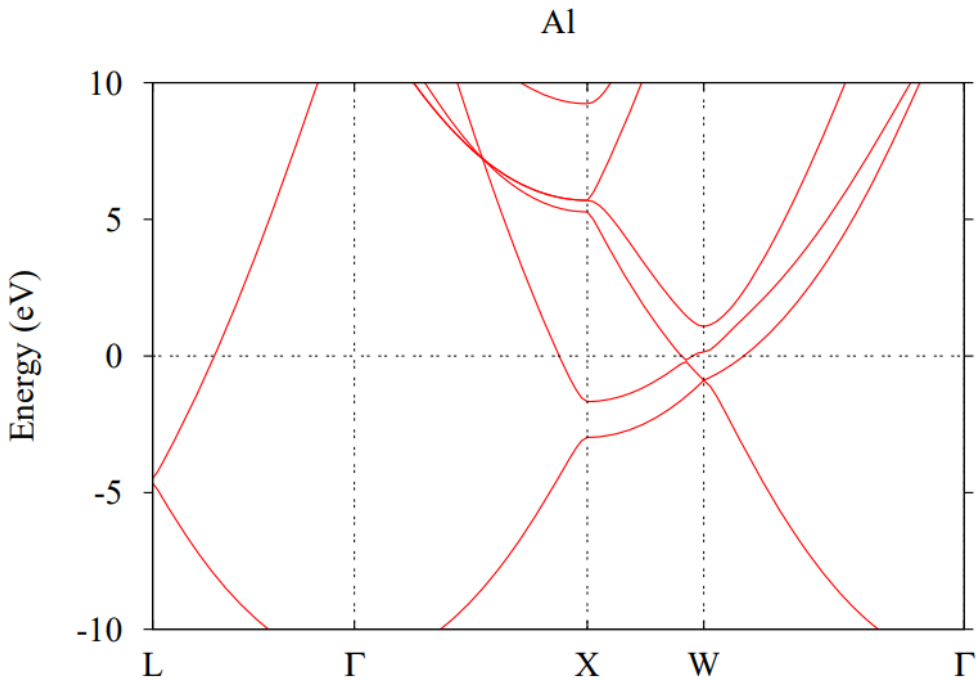


Figure 2: Aluminum band structure

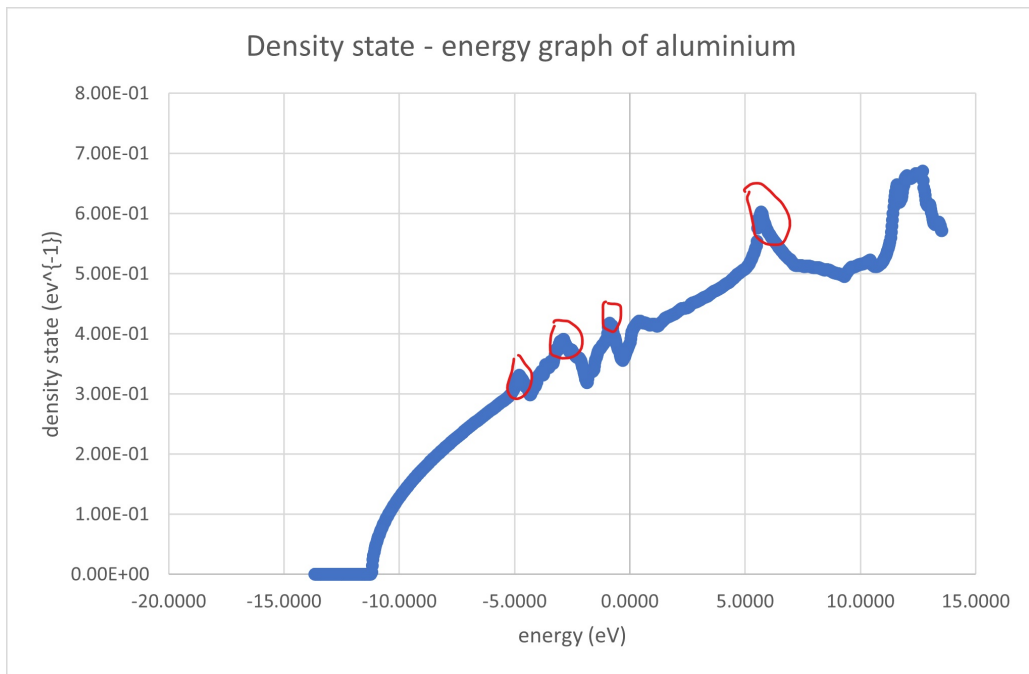


Figure 3: Density state - energy graph of aluminum. The red circles are van Hove singularities.

4.2 Result of silicon

4.2.1 Lattice constant

From figure 4, the lattice constant of silicon corresponding to the lowest cohesive energy is approximately

$$a_{Si} = 10.27 \text{ au} = 5.5458 \text{ \AA} \quad (2)$$

The obtained silicon lattice constant is approximately close to $a = 543.09 \text{ pm} = 5.4309 \text{ \AA}$ from <https://periodictable.com/Elements/014/data.html>.

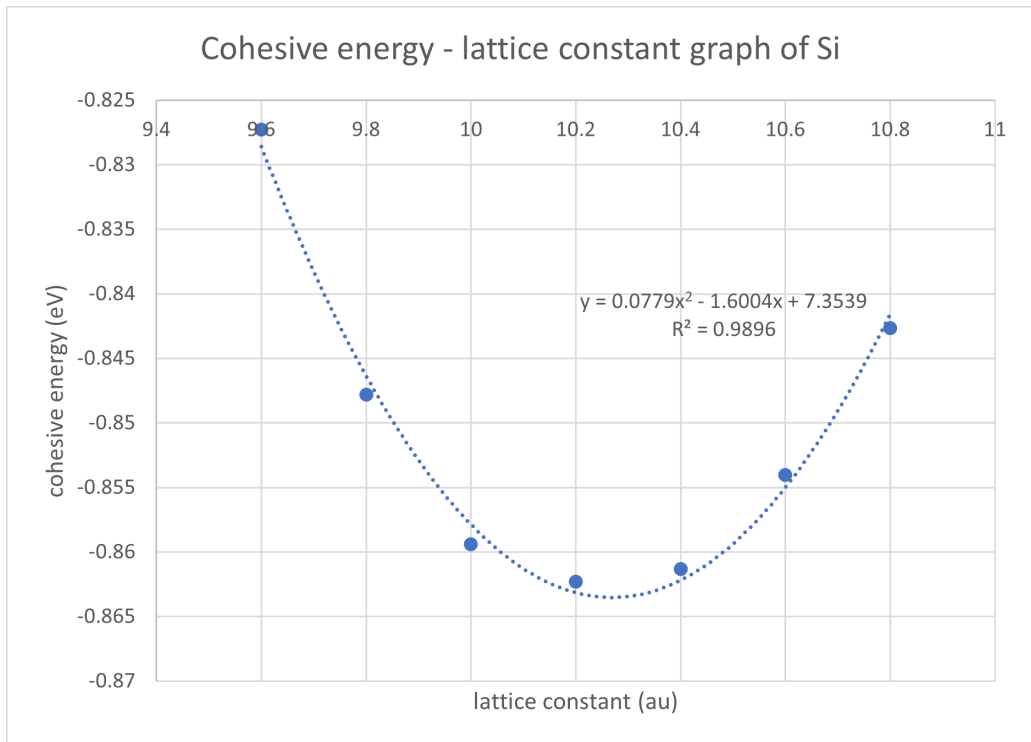


Figure 4: Lattice constant - cohesive energy graph of silicon

4.2.2 Density of state

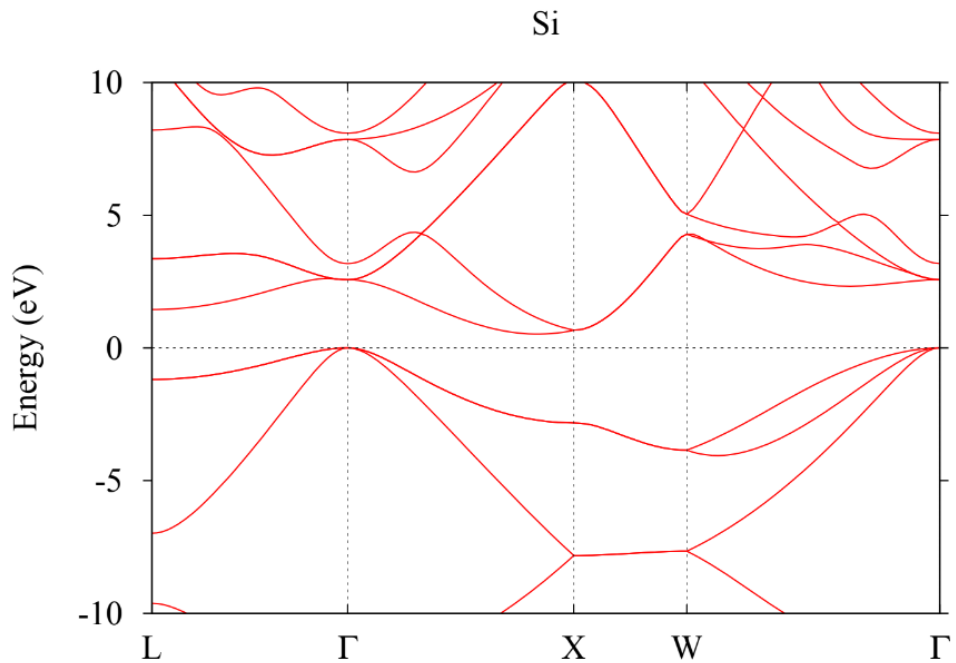


Figure 5: Silicon band structure

from figure 6 From a silicon band structure, the van Hove singularities are shown as peaks in the band structure.

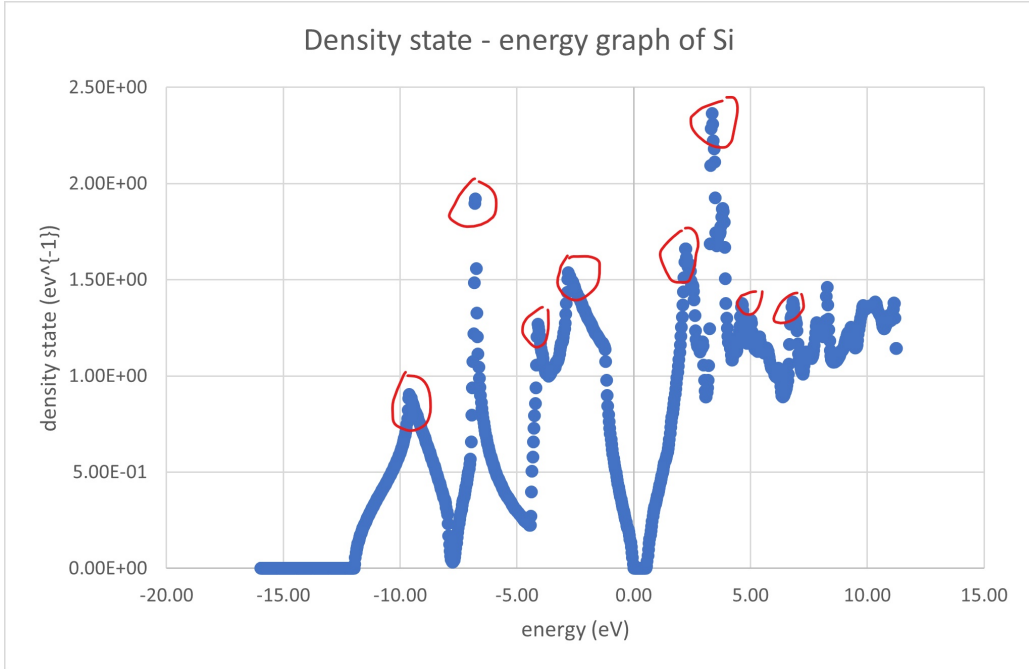


Figure 6: Density state - energy graph of silicon. The red circles are van Hove singularities.

4.3 Comparison of the results obtained from the aluminum and the silicon

Contrary to the aluminum DOS graph, there are a huge amount of van Hove singularities in the silicon DOS graph.

5 Conclusion

The experiment is to use density functional theory (DFT) to obtain the lattice constants of aluminum and silicon along with their band structure and visualization of the density of state (DOS). The computed lattice constant of aluminum is $a_{Al} = 4.019 \text{ \AA}$ and one of silicon is $a_{Si} = 5.5458 \text{ \AA}$. The band structures and DOS graph of both materials are constructed. The van Hove singularities are determined in both DOS graphs. From both DOS graph, there are a huge amount of van Hove singularities in the silicon DOS graph than one from the aluminum.